Check for updates

View Article Online
View Journal

ChemComm

Accepted Manuscript

This article can be cited before page numbers have been issued, to do this please use: G. Wang, Y. FU, Z. Ren, J. Huang, S. M. Best, X. Li and G.R. Han, *Chem. Commun.*, 2018, DOI: 10.1039/C8CC03480J.

This is an Accepted Manuscript, which has been through the Royal Society of Chemistry peer review process and has been accepted for publication.

Accepted Manuscripts are published online shortly after acceptance, before technical editing, formatting and proof reading. Using this free service, authors can make their results available to the community, in citable form, before we publish the edited article. We will replace this Accepted Manuscript with the edited and formatted Advance Article as soon as it is available.

You can find more information about Accepted Manuscripts in the author guidelines.

Please note that technical editing may introduce minor changes to the text and/or graphics, which may alter content. The journal's standard Terms & Conditions and the ethical guidelines, outlined in our author and reviewer resource centre, still apply. In no event shall the Royal Society of Chemistry be held responsible for any errors or omissions in this Accepted Manuscript or any consequences arising from the use of any information it contains.

ROYAL SOCIETY OF CHEMISTRY

rsc.li/chemcomm

Please do not adjust margins

View Article Online
DOI: 10.1039/C8CC03480J

Journal Name

COMMUNICATION

Upconversion nanocrystal 'armoured' silica fibres with superior photoluminescence for miRNA detection

Received 00th January 20xx,
Accepted 00th January 20xx

DOI: 10.1039/x0xx00000x

www.rsc.org/

Gang Wang[a], Yike Fu[a], Zhaohui Ren[a], Jie Huang[b], Serena Best[c] and Xiang Li[a]*, Gaorong Han[a]

We have fabricated a flexible membrane, consisting of SiO_2 nanofibres armoured with upconversion nanoparticles, exhibiting intense photoluminescence. These assemblies were subsequently grafted with molecular beacons to produce a biosensor suitable for the detection of specific microRNA and with applications in early cancer detection and point-of-care diagnosis.

MicroRNAs (miRNAs) dysfunction facilitates tumor growth, metastasis, angiogenesis, and immune evasion.[1, 2] The detection of cancer-related miRNAs, which present in body fluids, has been well recognized as a potential strategy for non-invasive early cancer diagnosis.[3, 4] Current approaches for miRNA detection fall into two main categories: biological testing methods (i.e. Northern blotting,[5] quantitative RT-qPCR[6, 7] and microarray assays[8, 9]) and chemical methods (i.e. electrochemical, fluorescent and electro-chemiluminescent platforms[10-12]). Fluorescence-based sensors, driven by the fluorescence resonance energy transfer (FRET) mechanism, have attracted considerable attention.[13-16] The FRET effect is related to the distance between the energy donor fluorophores and energy acceptor quenchers. In general, when the distance is below 10 nm, FRET occurs, and *vice versa*.

Upconversion luminescence nanomaterials have been explored for the construction of FRET-based miRNA detection biosensors owing to a number of intrinsic advantages, such as narrow emission peaks, long lifetime and superior photostability.[17-21] Photoluminescence nanofibres, where upconversion CaF_2 nanoparticles were incorporated within SiO_2 nanofibres via a particle electrospinning approach and subsequently grafted with miRNA capture probes, were investigated as a sensor for miRNA detection.[22] In the presence of target miRNA, the FRET effect is triggered and emission profiles can be used to assess the concentration of target miRNA. However, this particular type of upconversion nanoparticle(UCNP)-embedded nanofibres are poorly suited for clinical translation for miRNA detection due to their mechanical brittleness and limited sensitivity and selectivity. In contrast, UCNP-incorporated polymeric nanofibres have been reported as a type of alternative sensor.[23-25] However, the severe quenching by organic groups results in low intensity emission and poor sensitivity in biomarker detection. Therefore, there is a clear demand for an alternative technology based on flexible nanofibres with intense upconversion luminescence for biomarker detection.

Inspired by the flexible SiO_2 nanofibres achieved,[26] we hereby report the design and synthesis of a flexible membrane, consisting of SiO_2 nanofibres 'armoured' with upconversion nanoparticles (SiO_2@UCNP) for miRNA detection. (Fig 1) In this system, $NaYF_4$:Yb,Er upconversion nanoparticles were assembled at the surface of SiO_2 nanofibres (SiO_2@UCNP) via solvothermal growth. Carboxyl molecular beacons (MBs) with a Black Hole Quencher 3 (BHQ3) quencher were covalently

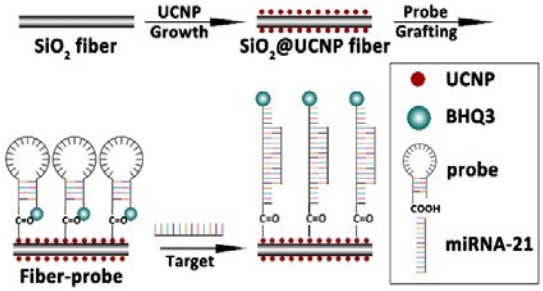

Fig. 1 Schematic illustration of the synthesis of SiO_2@UCNP-MB biosensor and miRNA detection.

[a] *State Key Laboratory of Silicon Materials, School of Materials Science and Engineering, Zhejiang University, Hangzhou, Zhejiang 310027, People's Republic of China.E-mail: xiang.li@zju.edu.cn, Tel/Fax: +86-0571-88276240*
[b] *Department of Mechanical Engineering, University College London, Torrington Place, London WC1E 7JE*
[c] *Department of Materials Science and Metallurgy, University of Cambridge, Cambridge CB3 0FS, UK*

Electronic Supplementary Information (ESI) available: SEM image and diameter distribution of SiO_2 nanofibres. TG analysis of electrospun PVA/SiO_2 nanofibres. Elemental mapping of SiO_2@UCNP nanofibres. TEM image and XRD pattern of $NaYF_4$:Yb,Er nanoparticles. Upconversion luminescence spectra of SiO_2@UCNP fibres and UCNP. SEM and TEM images of electrospun NaYF4:Yb,Er nanoparticles embedded SiO_2 nanofibres. See DOI: 10.1039/x0xx00000x

Published on 30 May 2018. Downloaded by Zhejiang University on 30/05/2018 03:10:33.

ChemComm Accepted Manuscript

Please do not adjust margins

View Article Online
DOI: 10.1039/C8CC03480J

Published on 30 May 2018. Downloaded by Zhejiang University on 30/05/2018 03:10:33.

grafted onto SiO_2@UCNP nanofibres. The red-light emission at 660 nm was quenched after MB immobilization. When the target miRNA presents, complementary co-hybridization between target and MB's loop sequence occurs and opens the hairpin structure, and the red-light emission at 660 nm recovered, resulting in the variation of intensity ratio I_{660}/I_{550} (spectrum at 660 nm to that at 550 nm).

Flexible SiO_2 fibres were synthesized by electrospinning based on modified protocol reported previously. [26] After calcination at 800 °C for 3 hours, SiO_2 nanofibres with smooth surface morphology and random porous structure, were prepared. (Fig. S1) No clear weight loss was observed when the samples were heated at above 800 °C, indicating the complete removal of PVA and the thermal stability of SiO_2 membrane (Fig. S2).[27] The inset optical micrograph shows a SiO_2 membrane wrapped around a test tube, demonstrating its flexibility (Fig. 2a).

After solvothermal growth of UCNP, the average diameter of SiO_2 nanofibres increased from ~380 nm to ~450 nm due to the assembly of UCNPs at the surfaces (Fig. 2a). TEM images show a uniform array of well-anchored UCNPs with a diameter of 30-50 nm (Fig. 2b). The high-resolution TEM (HRTEM) image reveals that the UCNPs comprised single crystals with clear lattice fringes with a d-spacing of 0.31 nm, corresponding to the (111) planes of the cubic $NaYF_4$:Yb,Er crystal (Fig. 2c). The XRD pattern of SiO_2@UCNP nanofibres shows a broad peak from 15° to 35° which is ascribed to amorphous SiO_2. All diffraction peaks on the trace match well with the characteristic pattern for α-$NaYF_4$:Yb,Er phase (JCPDS-77-2042), indicating an assembly of highly crystalline UCNPs on the surface of SiO_2 nanofibres. (Fig. 1d) The results of EDS mapping confirm the uniform and dense arrangement of UCNPs on the surface of nanofibres (Fig. S3). It was also observed that prolonged solvothermal time or reduced content of SiO_2 fibres during the synthesis may induce an assembly of increased content of UCNPs at the fibre surface (Fig S4).

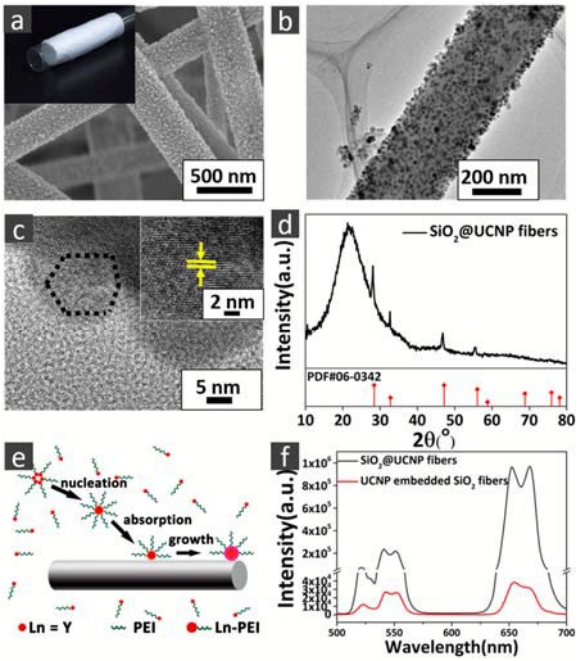

Fig. 2 (a) SEM, (b) TEM, (c) HRTEM images and (d) XRD pattern of SiO_2@UCNP fibres; (e) Illustration of growth mechanism of SiO_2@UCNP fibres; (f) Upconversion luminescence spectra of electrospun SiO_2@UCNP fibres and conventional UCNP embedded SiO_2 fibres reported previously.

For the formation of nanocrystals at the fibre surface, surfactants such as PVP, PEI are often used to guide the growth of the nanocrystals.[28] In this study, PEI was chosen as the surfactant owing to its positive charge. Initially, a Y-PEI complex is formed after inducing the Ln^{3+} solution. Subsequently, $NaYF_4$ nucleation occurs rapidly by the reaction of a mixture containing Y-PEI, NaCl and NH_4F, producing a white colloid solution (Fig. 2e). SiO_2 nanofibres are negatively charged due to the high content of Si-OH groups present at the surface. When immersing SiO_2 nanofibres in $NaYF_4$:Yb,Er precursor solution, $NaYF_4$ nuclei are adsorbed on the surface of the SiO_2 nanofibres via electrostatic attraction. $NaYF_4$ nucleus grow progressively to form $NaYF_4$ nanocrystals as the solvothermal process evolved. The Zeta potential consequently increases from -54 mV for SiO_2 nanofibres to ~56 mV of SiO_2@UCNP nanofibres, confirming the existence of the UCNPs attached with PEI groups (Fig. 3b). This model of a nucleation-adsorption-growth mechanism can be applied to explain the preparation of many SiO_2@nanocrystal complex nanofibres such as SiO_2@MnO_2, SiO_2@LDH and SiO_2@$NiFeO_4$ nanofibres. [29-31]

Intense upconversion luminescence of biosensors is a crucial characteristic for ensuring the sensitivity and selectivity of miRNA detection, especially in FRET based platforms. In this study, under irradiation using a 980 nm laser, the SiO_2@UCNP nanofibres exhibited two main upconversion luminescence (UCL) emissions. The green emission (550 nm) was induced by $(^2H_{11/2}, {}^4S_{3/2}) \rightarrow {}^4I_{15/2}$ transition, and the red emission was attributed to $^4F_{9/2} \rightarrow {}^4I_{15/2}$ transition, which is similar to that of $NaYF_4$:Yb,Er nanoparticles. (Fig. 2f) Notably, the UCL intensity of SiO_2@UCNP nanofibres was about 30-fold higher than that of $NaYF_4$:Yb,Er nanoparticles embedded SiO_2 nanofibres fabricated following the protocols reported previously[32], and comparable to that of pure $NaYF_4$:Yb,Er nanoparticles (Fig S5 & S6). The enhanced UCL intensity of SiO_2@UCNP nanofibres was attributed to the high density of UCNPs presented at the fibre surface and highly suppressed quenching effect by SiO_2 matrix. In contrast, for the UCL SiO_2 nanofibres reported previously[32], UCNPs are conventionally incorporated via a particle electrospinning method. The loading efficiency is limited because instability occurs when excessive particles are incorporated during electrospinning. Moreover, UCL emission of UCNP embedded and the excitation light are dramatically quenched by SiO_2 matrix. The 'armouring' of flexible SiO_2 nanofibres with UCNPs at the outer surface in this study has enabled the construction of UCL nanofibres with unique structural, mechanical and optical characteristics for biomarker detection and potentially localized photodynamic therapy.

Subsequently, carboxyl group-modified molecular beacons were immobilized on the surface of SiO_2@UCNP nanofibres via

ChemComm Accepted Manuscript

This journal is © The Royal Society of Chemistry 20xx

Please do not adjust margins
View Article Online
DOI: 10.1039/C8CC03480J

Published on 30 May 2018. Downloaded by Zhejiang University on 30/05/2018 03:10:33.

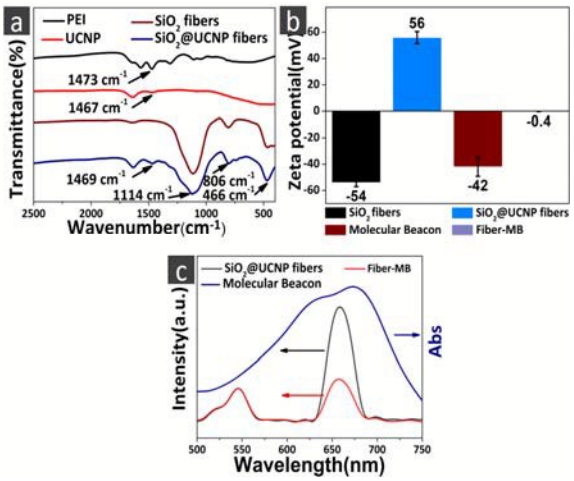

Fig. 3 (a) FTIR spectra of PEI, UCNP, SiO_2 fibres and SiO_2@UCNP fibres; (b) Zeta potentials of SiO_2 fibres, SiO_2@UCNP fibres, molecular beacons and SiO_2@UCNP-MB composite; (c) Upconversion luminescence spectra of SiO_2@UCNP fibres before and after molecular beacon grafting, and UV-vis spectrum of molecular beacons.

an amide reaction. As shown in Fig. 3a, the FTIR spectrum of the SiO_2 nanofibres reveals typical SiO_2 absorption bands at ~466 cm^{-1} for Si-O-Si bending vibration, at ~806 cm^{-1} for Si-O-Si symmetric stretching vibration and at ~1114 cm^{-1} for Si-O-Si asymmetric stretching vibration. Owing to UCNP assembly, a new peak at ~1470 cm^{-1}, which is assigned to N-H bending of secondary amines and -CH_2 scissoring vibrations of PEI, appears in the FTIR spectrum of SiO_2@UCNP nanofibres.[33] Accordingly, the increase of Zeta potential also confirms the presence of PEI. (Fig. 3b)

The UV-vis absorption of the molecular beacon shows a broad band at ~660 nm due to the BHQ3 quencher (Fig. 3c). After MB immobilization, emission of SiO_2@UCNP nanofibres at 660 nm was significantly quenched, resulting in a decrease in the intensity ratio of red emission to green light from 3.5 to 1.1. The conjugation of MB was further confirmed by the negative zeta potential of SiO_2@UCNP-MB composite resulting from the presence of negatively charged molecular beacon.

The FRET effect is closely related to the distance between the energy donor (UCNP on SiO_2@UCNP nanofibres) and acceptor (BHQ3). In general, the FRET effect occurs when the distance between the energy donor and acceptor is less than 10 nm. After molecular beacon immobilization, BHQ3 and UCNP were brought into close proximity, and the FRET phenomenon occurred, as reflected in Fig. 3c. For the miRNA detection examination, a membrane consisting of SiO_2@UCNP-MB fibres was immersed in a test tube containing 2 mL deionized water. When target miRNA solutions with known concentrations were added, the intensity ratio of I_{660} (intensity at 660nm) to I_{550} (intensity at 550 nm) recovered to 3.45 when the concentration of miRNA-21 reached 500 nM, indicating the successful restoration of red light emission (Figure 4a). The relationship between I_{660}/I_{550} (intensity ratio of red light to green light of SiO_2@UCNP-MB composite in the presence and absence of

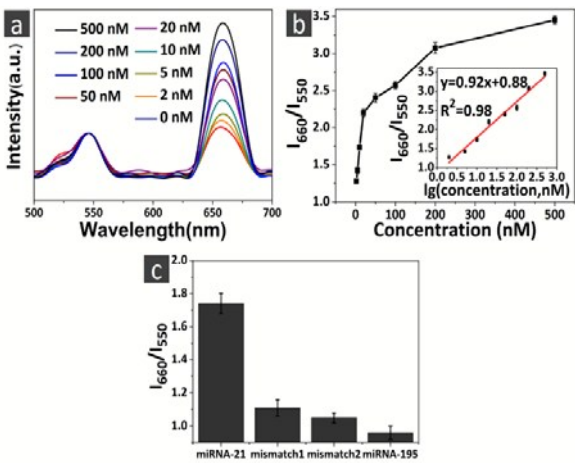

Fig. 4 (a) Upconversion luminescence spectra of SiO_2@UCNP-MB biosensor at different concentrations of miRNA-21; (b) relationship between the intensity ratio I_{660}/I_{550} and the concentration of miRNA-21; (c) specific detection of miRNA-21, miRNA-21 with single base mismatch, miRNA-21 with three bases mismatches and miRA-195.

target miRNA) and concentration of target miRNA (miRNA-21) is shown in Fig. 4b. I_{660}/I_{550} increased with the addition of target miRNA and varied with the concentration of miRNA-21 in a linear manner. The limit of detection was ~2 nM in DI water. This phenomenon is attributed to the co-hybridization which occurred between the target miRNA and the molecular beacon's loop sequence. When the target miRNA is presents, the hairpin structure is opened, and the quencher and UCNP are separated, enabling the recovery of emission of UCNP at 660 nm upon excitation. The selective detection of miRNA in a biological condition was verified using 10%vol fetal bovine serum. The I_{660}/I_{550} ratio presents in a linear relationship with miRNA-21 concentration when the miRNA-21 concentration varies from 50 nM to 500 nM. (Fig. S7 a&b) It is noted that the detection performance was weakened due to the interaction between protein molecules and Fibre-MB biosensor.[34]

A unique advantage of MBs-based biosensors is the high specificity due to the intrinsic hairpin structure.[35-36] Carcinogenesis is generally accompanied with a series of DNA mutations, and many miRNA family members only have one base mismatch difference. Thus, discriminating similar miRNA sequences is vital for cancer detection. To validate the specificity of SiO_2@UCNP-MB sensor, miRNA-21, miRNA-21

Table 1 Sequences of Molecular Beacons, miRNA-21, miRNA-195, mismatch1 and mismatch2.

Oligonucleotide name	Sequences (5'-3')
Molecular beacon	COOH-AGCGTCAACATCAGTCTGATAAGCTACGCT-BHQ3
miRNA-21	UAGCUUAUCAGACUGAUGUUGA
Mismatch 1	UAGCUUAUCCGACUGAUGUUGA
Mismatch 2	UAGCUUAUACUACUGAUGUUGA
miRNA-195	UAGCAGCACAGAAAUAUUGGC

ChemComm Accepted Manuscript

Please do not adjust margins

View Article Online
DOI: 10.1039/C8CC03480J

Published on 30 May 2018. Downloaded by Zhejiang University on 30/05/2018 03:10:33.

with single-base mismatch and three-base mismatch and miRNA-195, listed in Table 1, were synthesized and used for further test. As shown in Figure 4c, I_{660}/I_{550} ratio reaches 1.74 in the presence of 10 nM of miRNA-21, while this ratio maintains at 1.1 and 1.0 when 10 nM of miRNA-21 with single-base and three-base mismatch were added, respectively. In addition, the presence of miRNA-195 hardly induces variation of the I_{660}/I_{550} ratio, indicating detection specificity of the SiO_2@UCNP-MB fibres. In a fetal bovine condition, the biosensor presented certain discrimination among miRNA-21, one-base and three-base mismatched miRNA-21 and miRNA-195, demonstrating its detection specificity in biological environment. (Fig. S7 c&d)

In summary, $NaYF_4$:Yb,Er nanoparticles were assembled on the surface of flexible SiO_2 nanofibre following a nucleation-adsorption-growth mechanism. The 'armoured' fibres exhibit high intensity of upconversion luminescence at 550 nm and 660 nm owing to high content of UCNPs incorporated and suppressed quenching by amorphous SiO_2 matrix. When grafted with molecular beacons, the FRET effect is triggered and the emission at 660 nm is significantly reduced by the quencher in the MB molecules. In the presence of target miRNA, the complementary co-hybridization between target sequence and the loop sequence of the molecular beacon opens the hairpin structure and the emission at 660 nm recovered, enabling the quantitative detection of target miRNA concentration. The limit of detection reaches ~2 nM while the specificity is ensured. Comparing to current photoluminescence detection schemes, this membrane of armoured nanofibres, presenting superior UCL, mechanical flexibility for practical operation and unique detection properties, is therefore anticipated to offer considerable potential as a biosensor in early cancer diagnosis and therapy.

Acknowledgements

This work was financially supported by the National Nature Science Foundation of China (51672247), the '111' Program funded by Education Ministry of China and State Administration of Foreign Experts Affairs (B16043), the Major State Research Program of China (2016YFC1101900).

Notes and references

1 Y. Choudhury, F. C. Tay, D. H. Lam, E. Sandanaraj, C. Tang, B. T. Ang and S. Wang, *J. Clin. Invest.*, 2012, **122**, 4059-4076.
2 C. Stahlhut and F. J. Slack, *Genome Med.*, 2013, **5**, 12.
3 X. Chen, Y. Ba, L. J. Ma, X. Cai, Y. Yin, K. H. Wang, J. G. Guo, Y. J. Zhang, J. N. Chen, X. Guo, Q. B. Li, X. Y. Li, W. J. Wang, Y. Zhang, J. Wang, X. Y. Jiang, Y. Xiang, C. Xu, P. P. Zheng, J. B. Zhang, R. Q. Li, H. J. Zhang, X. B. Shang, T. Gong, G. Ning, J. Wang, K. Zen, J. F. Zhang and C. Y. Zhang, *Cell Res.*, 2008, **18**, 997-1006.
4 J. B. Li, S. B. Tan, R. Kooger, C. Y. Zhang and Y. Zhang, *Chem. Soc. Rev.*, 2014, **43**, 506-517.
5 G. S. Pall, C. Codony-Servat, J. Byrne, L. Ritchie and A. Hamilton, *Nucleic Acids Res.*, 2007, **35** ,60.
6 X. Liao, Q. Wang and H. Ju, *Chem. Commun.*, 2014, **50**, 13604-13607.
7 J. Li, B. Yao, H. Huang, Z. Wang, C. Sun, Y. Fan, Q. Chang, S. Li, X. Wang and J. Xi, *Anal. Chem.*, 2009, **81**, 5446-5451.
8 P. T. Nelson, D. A. Baldwin, L. M. Scearce, J. C. Oberholtzer, J. W. Tobias and Z. Mourelatos, *Nat. Methods*, 2004, **1**, 155-161.
9 J. M. Lee and Y. Jung, *Angew. Chem. Int. Ed.*, 2011, **50**, 12487-12490.
10 S. Campuzano, M. Pedrero and J. M. Pingarron, *Anal. Bioanal Chem.*, 2014, **406**, 27-33.
11 Y. Cheng, J. Lei, Y. Chen and H. Ju, *Biosens. Bioelectron.*, 2014, **51**, 431-436.
12 F. Causa, A. Aliberti, A. M. Cusano, E. Battista and P. A. Netti, *J. Am. Chem. Soc.*, 2015, **137**, 1758-1761.
13 Z. L. Qiu, J. Shu and D. P. Tang, *Anal. Chem.,* 2017, **89**, 5152−5160.
14 Z. Jin, D. Geissler, X. Qiu, K. D. Wegner and N. Hildebrandt, *Angew. Chem. Int. Ed.*, 2015, **54**, 10024-10029.
15 Z. L. Qiu, J. Shu and D. P. Tang, *Anal. Chem.,* 2018, **90**, 1021−1028
16 J. A. M. Vet, A. R. Majithia, S. A. E. Marras, S. Tyagi, S. Dube, B. J. Poiesz and F. R. Kramer, *Proc. Natl. Acad. Sci U.S.A.*, 1999, **96**, 6394-6399.
17 L. Wang, J. Liu, Y. Dai, Q. Yang, Y. Zhang, P. Yang, Z. Cheng, H. Lian, C. Li, Z. Hou, P. a. Ma and J. Lin, *Langmuir*, 2014, **30**, 13042-13051.
18 Y. Fu, C. Fang, Z. Ren, G. Xu, X. Li and G. Han, *Chem.-Eur. J.*, 2017, **23**, 2423-2431.
19 Z. L. Qiu, J. Shu, Y. Hen, Z. Z. Lin, K. Y. Zhang, S. Z. Lv and D. P. Tang, *Biosens. and Bioelectron.,* 2017, **87**, 18–24.
20 Z. Z. Lin, S. Z. Lv, K. Y. Zhang and D. P. Tang, *J. Mater. Chem. B,* 2017, **5**, 826-833
21 H. Du, J. Yu, D. Guo, W. Yang, J. Wang and B. Zhang, *Langmuir*, 2016, **32**, 1155-1165.
22 Y. K. Fu, T. Chen, G. Wang, T. Gu, C. Xie, J. Huang, X. Li, S. Best and G. Han, *J. Mater. Chem. B*, 2017, **5**, 7133-7139.
23 K. C. Liu, Z. Y. Zhang, C. X. Shan, Z.-Q. Feng, J. S. Li, C. L. Song, Y. N. Bao, X. H. Qi and B. Dong, Light-Sci. Appl., 2016, **5**.
24 P. Zou, X. Hong, Y. Ding, Z. Zhang, X. Chu, T. Shaymurat, C. Shao and Y. Liu, *J. Phys. Chem. C*, 2012, **116**, 5787-5791.
25 Z. Hou, X. Li, C. Li, Y. Dai, P. a. Ma, X. Zhang, X. Kang, Z. Cheng and J. Lin, *Langmuir*, 2013, **29**, 9473-9482.
26 Y. Si, X. Mao, H. Zheng, J. Yu and B. Ding, *RSC Adv.*, 2015, **5**, 6027-6032.
27 X. Mao, Y. Si, Y. Chen, L. Yang, F. Zhao, B. Ding and J. Yu, *RSC Adv.*, 2012, **2**, 12216-12223.
28 J. Zhao, X. Liu, D. Cui, Y. Sun, Y. Yu, Y. Yang, C. Du, Y. Wang, K. Song, K. Liu, S. Lu, X. Kong and H. Zhang, *Eur. J. Inorg. Chem.*, 2010, **12**, 1813-1819.
29 W. Lv, Q. Mei, H. Fu, J. Xiao, M. Du and Q. Zheng, *J. Mater. Chem. A*, 2017, **5**, 19079-19090.
30 X. Wang, L. Dou, L. Yang, J. Yu and B. Ding, *J. Hazard. Mater.*, 2017, **324**, 203-212.
31 F. Hong, C. Yan, Y. Si, J. He, J. Yu and B. Ding, *Acs Appl. Mater. Inter.*, 2015, **7**, 20200-20207.
32 Z. Hou, C. Li, P. Ma, G. Li, Z. Cheng, C. Peng, D. Yang, P. Yang and J. Lin, *Adv. Funct. Mater.*, 2011, **21**, 2356-2365.
33 A. Paciello and M. G. Santonicola, *RSC Adv.*, 2015, **5**, 88866-88875.
34 W. L. Ren, G. Tian, S. Jian, Z. J. Gu, L. J. Zhou, L. Yan, S. Jin, W. Y. Yin and Y. L. Zhao, *RSC Adv.*, 2012, **2**, 7037-7041
35 G. Bonnet, S. Tyagi, A. Libchaber, and F. R. Kramer, *Proc. Natl. Acad. Sci.*, 1999, **96**, 6171–6176.
36 S. Tyagi, D. P. Bratu and Fred Russell Kramer, *Nat. Biotechnol.*, 1998, **6**, 49-53.

ChemComm Accepted Manuscript

This journal is © The Royal Society of Chemistry 20xx